

## Pion and nucleon in two flavour QCD with unimproved Wilson fermions

---

Abhishek Chowdhury<sup>a</sup>, Asit K. De<sup>a</sup>, Sangita De Sarkar<sup>a</sup>, A. Harindranath<sup>a</sup>, Jyotirmoy Maiti<sup>b</sup>, Santanu Mondal<sup>a</sup> and Anwesa Sarkar<sup>a</sup>

<sup>a</sup>*Theory Division, Saha Institute of Nuclear Physics  
1/AF Bidhan Nagar, Kolkata 700064, India*

<sup>b</sup>*Department of Physics, Barasat Government College,  
10 KNC Road, Barasat, Kolkata 700124, India*

*E-mail:* [abhishek.chowdhury@saha.ac.in](mailto:abhishek.chowdhury@saha.ac.in), [asitk.de@saha.ac.in](mailto:asitk.de@saha.ac.in),  
[sangita.desarkar@saha.ac.in](mailto:sangita.desarkar@saha.ac.in), [a.harindranath@saha.ac.in](mailto:a.harindranath@saha.ac.in),  
[jyotirmoy.maiti@gmail.com](mailto:jyotirmoy.maiti@gmail.com), [santanu.mondal@saha.ac.in](mailto:santanu.mondal@saha.ac.in),  
[anwesa.sarkar@saha.ac.in](mailto:anwesa.sarkar@saha.ac.in)

ABSTRACT: We calculate pion mass, pion decay constant, PCAC quark mass and nucleon mass in two flavour lattice QCD with unimproved Wilson fermion and gauge actions. Simulations are performed using DD-HMC algorithm at two lattice spacings and two volumes for several values of the quark mass. The cutoff effects in pion mass and nucleon mass for the explored region of parameter space are found to be negligible. The chiral behaviours of pion mass, pion decay constant and quark condensate are found to be qualitatively consistent with NLO chiral perturbation theory.

---

## Contents

<b>1</b>	<b>Introduction</b>	<b>1</b>
<b>2</b>	<b>Simulation and Observables</b>	<b>2</b>
<b>3</b>	<b>Computation of pion mass and decay constant, PCAC quark mass and nucleon mass</b>	<b>4</b>
<b>4</b>	<b>Determination of <math>\frac{r_0}{a}</math></b>	<b>6</b>
<b>5</b>	<b>Cutoff effects</b>	<b>8</b>
<b>6</b>	<b>Scale determination, chiral behaviour of nucleon mass and extraction of sigma term</b>	<b>10</b>
<b>7</b>	<b>Chiral extrapolations of pion mass and decay constant and quark condensate</b>	<b>12</b>
<b>8</b>	<b>Summary</b>	<b>15</b>

---

## 1 Introduction

Because of the explicit violation of chiral symmetry by a dimension five kinetic operator, Wilson formulation has been known to be difficult to simulate at light quark masses. Lack of chiral symmetry means that the “physical” quark mass is no longer proportional to the bare quark mass (the quark mass renormalization is no longer only multiplicative) and Wilson-Dirac operator is not protected from arbitrarily small eigenvalues and may lead to zero or near zero modes for individual configurations. This is the infamous problem of “exceptional configurations”. This leads to convergence difficulties for fermion matrix inversion. This poses difficulties for lattice simulations with Wilson fermions in the chiral region.

In the past, simulations with unimproved Wilson action has shown large scaling violations in hadronic observables. However, one should keep in mind that most of these were quenched simulations done at large pion masses, not small enough lattice spacings and smaller volumes. Further, the demonstration of the suppression of topological susceptibility with decreasing quark mass was inconclusive. The chiral behaviour of pion mass and decay constant with respect to quark mass (specifically, the presence of chiral logarithms) as dictated by chiral perturbation theory was also not convincingly demonstrable in the past with un-improved Wilson fermions. All these issues raise the question: Does Wilson lattice QCD belong to the same universality class as continuum QCD?

The situation regarding “exceptional configurations” has improved partly due to the finding [2] employing DD-HMC algorithm [3] that the numerical simulations are safe from accidental zero modes for large volumes. Simulations with unimproved Wilson fermions at smaller quark masses and lattice spacings and larger volumes have become possible with the DD-HMC algorithm. As

part of an on-going program [4, 5] to study the chiral properties of Wilson lattice QCD (unimproved fermion and gauge actions), recently, we have demonstrated the suppression of topological susceptibility with decreasing quark mass in the case of unimproved Wilson fermion and gauge action [6, 7] where, the suppression of topological susceptibility with decreasing volume was also shown. In order to shed light on the mechanisms leading to these suppressions, we have further carried out a detailed study of the two-point topological charge density correlator [8]. An exploratory investigation of the autocorrelations of various observables with DD-HMC algorithm is presented in Ref. [9]. In these works we have employed ensembles of gauge configurations generated by means of DD-HMC [3] algorithm using unimproved Wilson fermion and Wilson gauge actions [1] with  $n_f = 2$  mass degenerate quark flavours.

In this work we investigate pion mass ( $m_\pi$ ) and decay constant, PCAC quark mass, quark condensate and nucleon mass in the range  $290 \lesssim m_\pi \lesssim 750$  MeV. We perform qualitative chiral extrapolations of various observables in the range  $350 \lesssim m_\pi \lesssim 550$  MeV. So far the simulations are done at two lattice spacings in the region of 0.05 - 0.07 fm where many of the modern simulations of LQCD with improved actions are carried out.

## 2 Simulation and Observables

Simulations have been carried out at two values of the gauge coupling correspond to  $\beta=5.6$  and 5.8. At  $\beta = 5.6$  the lattice volumes are  $24^3 \times 48$  and  $32^3 \times 64$  and at  $\beta = 5.8$  the lattice volume is  $32^3 \times 64$ . The number of thermalized gauge configurations ranges from 3760 to 13646. The lattice parameters and simulation statistics are given in Table 1. For all ensembles of configurations the average Metropolis acceptance rates range between 75 – 98%. For pion and nucleon we consider the following zero spatial momentum correlation functions

$$C(t) = \langle 0 | \mathcal{O}_1(t) \mathcal{O}_2(0) | 0 \rangle \quad (2.1)$$

where  $t$  refers to Euclidean time. For the nucleon  $\mathcal{O}_1 \mathcal{O}_2 \equiv N \bar{N}$  with  $N = (q_d^T C \gamma_5 q_u) q_u$ . For the pion  $\mathcal{O}_1 \mathcal{O}_2 \equiv PP^\dagger, AA^\dagger, AP^\dagger$  or  $PA^\dagger$  where  $P = \bar{q}_i \gamma_5 q_j$  (pseudoscalar density) and  $A$  corresponds to  $A_4 = \bar{q}_i \gamma_4 \gamma_5 q_j$  (fourth component of the axial vector current). Here  $i$  and  $j$  stand for flavor indices for the  $u$  and  $d$  quarks and for the charged pion  $i \neq j$ . For pion we use point source and point sink and for nucleon we use wall source and point sink. Unless otherwise stated 20 HYP smearing steps with optimized smearing coefficients  $\alpha_1 = 0.75$ ,  $\alpha_2 = 0.6$  and  $\alpha_3 = 0.3$  [10] are used for the gauge observables.

The pion decay constant  $F_\pi$  and the quark mass  $m_q$  from PCAC or the axial Ward identity (AWI) are respectively defined, in the continuum as follows:

$$\langle 0 | A_\mu(0) | \pi(p) \rangle = F_\pi p_\mu, \quad (2.2)$$

$$\partial_\mu A_\mu(x) = 2m_q P(x). \quad (2.3)$$

From the PP and the AP propagators

$$C^{PP} = \frac{1}{2m_\pi} | \langle 0 | P(0) | \pi \rangle |^2, \quad (2.4)$$

$$C^{AP} = \frac{1}{2m_\pi} \langle 0 | A_4(0) | \pi \rangle \langle \pi | P^\dagger(0) | 0 \rangle \quad (2.5)$$

$\beta = 5.6$

<i>tag</i>	<i>lattice</i>	$\kappa$	<i>block</i>	$N_2$	$N_{cfg}$	$\tau$	$r_0 \times m_\pi$
$B_{1b}$	$24^3 \times 48$	0.1575	$12^2 \times 6^2$	18	13128	0.5	1.7719(38)
$B_{3b}$	,,	0.158	$12^2 \times 6^2$	18	13646	0.5	1.2542(58)
$B_{4b}$	,,	0.158125	$12^2 \times 6^2$	18	11328	0.5	1.0925(58)
$C_1$	$32^3 \times 64$	0.15775	$8^3 \times 16$	8	6844	0.5	1.5345(54)
$C_2$	,,	0.158	$8^3 \times 16$	8	7576	0.5	1.2590(59)
$C_3$	,,	0.158125	$8^3 \times 16$	8	8768	0.5	1.1010(60)
$C_4$	,,	0.15815	$8^3 \times 16$	8	9556	0.5	1.0697(57)
$C_5$	,,	0.15825	$8^3 \times 16$	8	11520	0.5	0.9343(55)
$C_6$	,,	0.1583	$8^3 \times 16$	8	4384	0.25	0.8476(99)

$\beta = 5.8$

<i>tag</i>	<i>lattice</i>	$\kappa$	<i>block</i>	$N_2$	$N_{cfg}$	$\tau$	$r_0 \times m_\pi$
$D_{1a}$	$32^3 \times 64$	0.1543	$8^3 \times 16$	8	9600	0.5	1.3259(76)
$D_{2b}$	,,	0.15445	$8^3 \times 16$	24	4800	0.5	1.1138(73)
$D_{3a}$	,,	0.15455	$8^3 \times 16$	8	12160	0.5	0.9968(87)
$D_{4b}$	,,	0.15462	$8^3 \times 16$	24	7528	0.5	0.8637(81)
$D_{5b}$	,,	0.15466	$8^3 \times 16$	24	3760	0.5	0.8360(131)
$D_{6b}$	,,	0.1547	$8^3 \times 16$	24	4256	0.5	0.6851(181)

**Table 1.** Lattice parameters, simulation statistics and pion mass ( $m_\pi$ ) in the unit of Sommer parameter ( $r_0$ ). Here *block*,  $N_2$ ,  $N_{cfg}$ ,  $\tau$  refers to DD-HMC block, step number for the force  $F_2$ , number of DD-HMC configurations and the Molecular Dynamics trajectory length respectively.

which lead to

$$F_\pi^{AP} = \frac{2\kappa C^{AP}}{\sqrt{m_\pi C^{PP}}}. \quad (2.6)$$

Using PCAC

$$\partial_\mu \langle 0 | A_\mu(x) P^\dagger(0) | 0 \rangle = 2m_q \langle 0 | P(x) P^\dagger(0) | 0 \rangle. \quad (2.7)$$

Summing over spatial coordinates

$$\sum_{\mathbf{x}} \partial_\mu \langle 0 | A_\mu(x) P^\dagger(0) | 0 \rangle = 2m_q \sum_{\mathbf{x}} \langle 0 | P(x) P^\dagger(0) | 0 \rangle. \quad (2.8)$$

At large  $t$ ,

$$\partial_4 C^{AP} \left[ e^{-m_\pi t} - e^{-m_\pi(T-t)} \right] = 2m_q C^{PP} \left[ e^{-m_\pi t} + e^{-m_\pi(T-t)} \right] \quad (2.9)$$

which leads to

$$m_q^{AP} = \frac{m_\pi}{2} \frac{C^{AP}}{C^{PP}}. \quad (2.10)$$

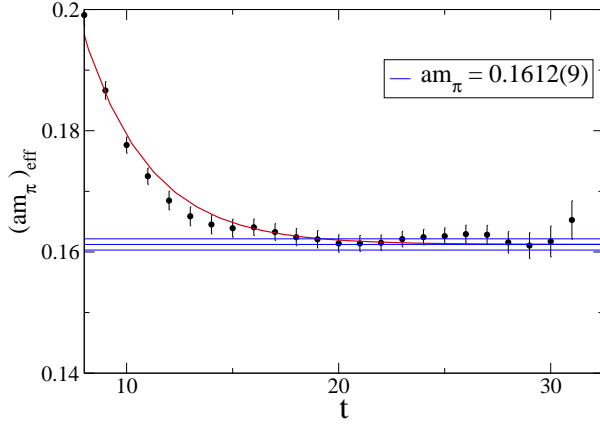


**Figure 1.** Effective mass  $am_\pi$  versus  $t$  for  $\beta = 5.8$ ,  $\kappa = 0.1543$  and the volume  $32^3 \times 64$ .

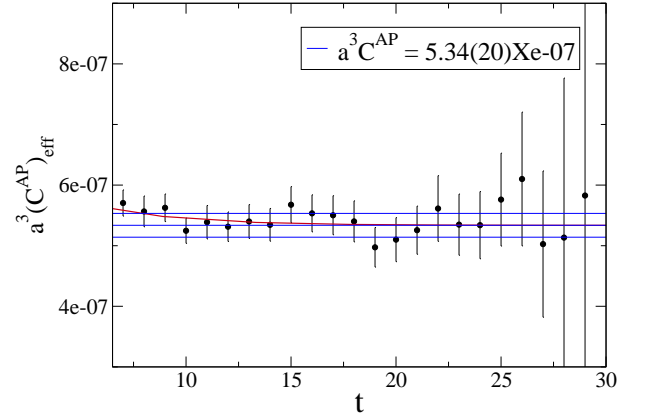
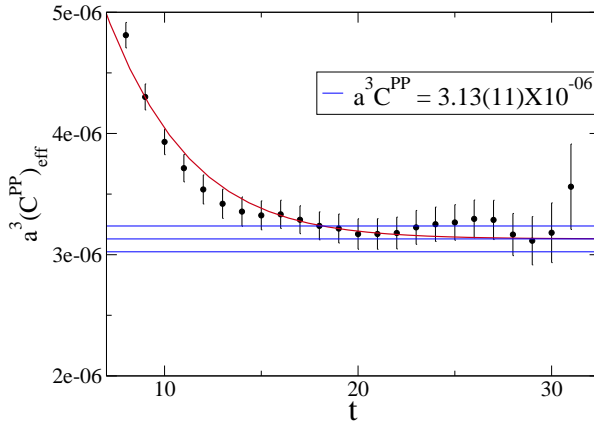


**Figure 2.** Effective coefficients  $a^3C_{PP}$  (left) and  $a^3C_{AP}$  (right) versus  $t$  for  $\beta = 5.8$ ,  $\kappa = 0.1543$  and the volume  $32^3 \times 64$ .

### 3 Computation of pion mass and decay constant, PCAC quark mass and nucleon mass

The two point correlation function  $C(t)$  (with point source and point sink) may be expanded as

$$C(t) = c_0 e^{-M_0 t} + c_1 e^{-M_1 t} + \dots \quad (3.1)$$

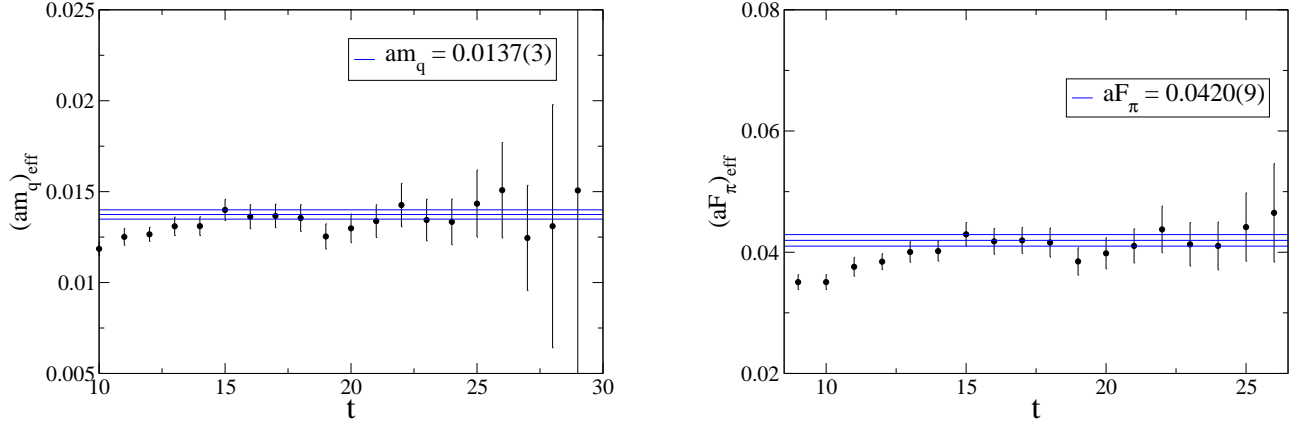


**Figure 3.** Effective  $am_q^{AP}$  and effective  $aF_\pi^{AP}$  versus  $t$  for  $\beta = 5.8$ ,  $\kappa = 0.1543$  and the volume  $32^3 \times 64$ .

where  $M_0$  denotes the mass of the ground state and  $M_1$  is the mass of the first excited state. The effective mass and the effective coefficient are given by

$$M_{eff}(t) = M_0 \left[ 1 + \frac{2c_1}{c_0} e^{-(M_1 - M_0)t} \right] \quad (3.2)$$

$$C_{eff}(t) = c_0 \left[ 1 + \frac{c_1}{c_0} (1 + 2M_0 t) e^{-2M_0 t} \right] \quad (3.3)$$

We first calculate effective pion mass  $(a(m_\pi)_{eff})$  from both  $PP$  and  $AP$  correlators. Then Eq. (3.2) is used to determine the asymptotic value  $aM_0$  of  $aM_{eff}(t)$ . Similarly we determine the asymptotic values of  $a^3 C^{PP}$  and  $a^3 C^{AP}$  by fitting  $a^3 C_{eff}^{PP}$  and  $a^3 C_{eff}^{AP}$  respectively with the Eq. (3.3).

The sample plots illustrating the dependence of these observables on  $t$  are given in figures 1 and 2 for  $\beta = 5.8$ ,  $\kappa = 0.1543$  and the volume  $32^3 \times 64$ . The fitting ranges in  $t$  are 8-31 and 8-29 for  $PP$  and  $AP$  correlators respectively. In these figures the horizontal line with error bars represent the asymptotic value giving the mass and coefficients.

The effective quark mass and the effective pion decay constant are calculated by using Eq. (2.10) and Eq. (2.6) respectively. The sample plots illustrating the dependence of  $(am_q^{AP})_{eff}$  and  $(aF_\pi^{AP})_{eff}$  on  $t$  are given in figure 3 for  $\beta = 5.8$ ,  $\kappa = 0.1543$  and the volume  $32^3 \times 64$ . In these figures the horizontal line with error bars represent the quark mass  $am_q^{AP}$  and pion decay constant  $aF_\pi^{AP}$  calculated using the asymptotic values of the mass and coefficients from Eq. (2.10) and Eq. (2.6).

We have extracted nucleon mass using wall source. Plots of the effective mass of nucleon at  $\beta=5.6$ , lattice volume  $24^3 \times 48$  and  $\kappa= 0.1575, 0.15775$  are shown in the Fig. 4 (left) where the fitting ranges are  $t = 11-16$  and  $11-14$  respectively. Similarly in Fig. 4 (right) we have shown the effective mass of nucleon at  $\beta=5.8$ , lattice volume  $32^3 \times 64$  for  $\kappa= 0.1543$  and  $0.15462$  with fitting ranges  $t = 9-25$  and  $16-20$  respectively. The effective masses are extracted from the linear fit to the plateau region. In table 2 we present the lattice data for  $am_\pi$ ,  $am_q$ ,  $aF_\pi$  and  $am_N$ . At  $\kappa = 0.15466$  for  $\beta = 5.8$ , the signal for effective mass of the nucleon was noisy so we do not quote a number.

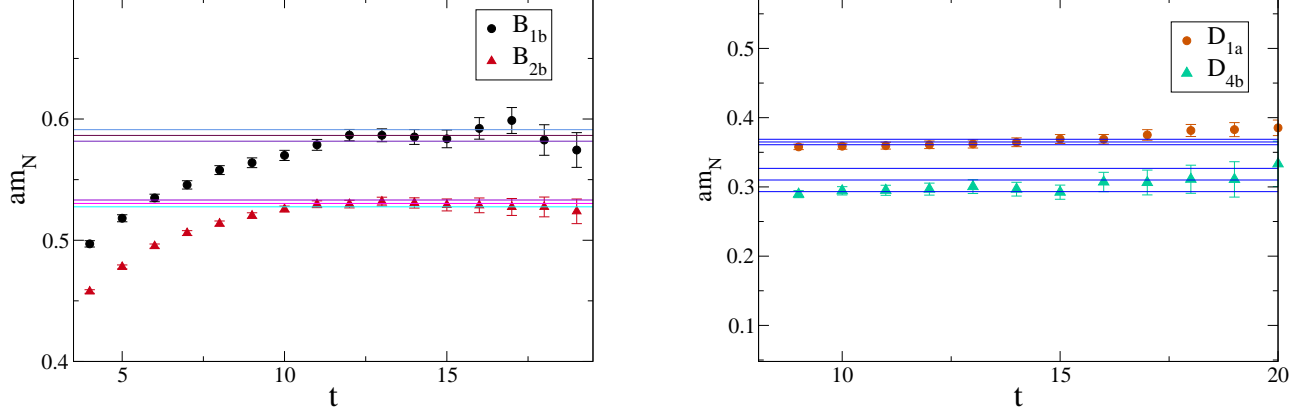


**Figure 4.** Typical plots of nucleon effective mass at  $\beta=5.6$  (left) and  $\beta=5.8$  (right).

From table 2 it is clear that finite volume effect is negligible for the pion mass and nucleon mass at  $\beta=5.6$  and lattice volume  $24^3 \times 48$ . At  $\beta=5.6$  and lattice volume  $32^3 \times 64$  for lightest quark masses studied  $m_\pi L$  values are 4.67 and 4.23 for  $\kappa = 0.15825$  and  $0.1583$  respectively. Note that the physical volume at  $\beta=5.6$  and lattice volume  $24^3 \times 48$  is very close to the physical volume at  $\beta=5.8$  and lattice volume  $32^3 \times 64$ . Thus comparing the values of  $r_0 m_\pi$  from table 1 for  $\beta=5.8$  we expect that finite volume effect should be negligible upto and including  $\kappa = 0.15455$  at lattice volume  $32^3 \times 64$ . At  $\beta=5.8$  for  $\kappa = 0.15462$  and  $0.15466$  the  $m_\pi L$  values are 3.36 and 3.25 respectively. Only for the smallest quark mass ( $\kappa = 0.1547$ )  $m_\pi L = 2.67$ . Hence qualitatively we expect that finite volume effect would be negligible for pion mass and nucleon mass for the region of parameter space studied except possibly for the lightest quark mass at  $\beta=5.8$ . According to NLO Chiral Perturbation Theory ( $\chi$ PT), the finite volume effect for  $F_\pi$  is four times that of  $m_\pi$ . Thus at  $\beta=5.8$  for  $\kappa = 0.15462$  and higher we can expect non negligible finite volume effect for  $F_\pi$ .

#### 4 Determination of $\frac{r_0}{a}$

We measured the Wilson loops  $\langle W(R, T) \rangle$  with temporal extents up to  $T = 32$  (24) and spatial separations up to  $R = \sqrt{3} \times 16$  ( $\sqrt{3} \times 12$ ) for lattice volume  $32^3 \times 64$  ( $24^3 \times 48$ ).

A reasonable estimate of the static potential  $aV(R)$  is obtained by the plateau reached at large  $T$  of the *effective* potential

$$aV_{\text{eff}}(R, T) = \ln \frac{\langle W(R, T) \rangle}{\langle W(R, T+1) \rangle}. \quad (4.1)$$

Phenomenologically, the potential  $V$  between a static quark and an antiquark at a distance  $r$  apart is parametrized as follows:  $V(r) = V_0 + \sigma r + \frac{\alpha}{r}$  where  $\sigma$  is the string tension which has the dimension of mass<sup>2</sup>. In lattice units, we have  $aV(r) = aV_0 + a^2 \sigma \frac{r}{a} + \alpha \frac{a}{r}$ . Writing  $r = Ra$  and  $\sigma = \tilde{\sigma}/a^2$ , we get  $aV(R) = aV_0 + \tilde{\sigma}R + \frac{\alpha}{R}$ .

$\beta = 5.6$

<i>lattice</i>	$\kappa$	$am_\pi$	$am_q$	$aF_\pi$	$am_N$
$24^3 \times 48$	0.1575	0.2764(6)	0.0277(3)	0.0655(7)	0.5865(48)
,,	0.158	0.1957(9)	0.0148(3)	0.0549(12)	0.4735(65)
,,	0.158125	0.1704(9)	0.0110(3)	0.0502(13)	0.4450(18)
$32^3 \times 64$	0.15775	0.2394(8)	0.0211(2)	0.0599(9)	0.5304(28)
,,	0.158	0.1964(9)	0.0145(2)	0.0543(10)	0.4676(51)
,,	0.158125	0.1718(9)	0.0111(2)	0.0503(10)	0.4389(134)
,,	0.15815	0.1669(9)	0.0110(3)	0.0511(15)	0.4425(64)
,,	0.15825	0.1458(9)	0.0078(1)	0.0474(9)	0.4045(61)
,,	0.1583	0.1322(15)	0.0063(2)	0.0452(11)	0.4024(268)

$\beta = 5.8$

<i>lattice</i>	$\kappa$	$am_\pi$	$am_q$	$aF_\pi$	$am_N$
$32^3 \times 64$	0.1543	0.1612(9)	0.0137(3)	0.0420(9)	0.3649(39)
,,	0.15445	0.1355(9)	0.0096(3)	0.0366(11)	0.3418(40)
,,	0.15455	0.1212(11)	0.0074(3)	0.0344(15)	0.3308(63)
,,	0.15462	0.1050(10)	0.0055(2)	0.0328(12)	0.3100(168)
,,	0.15466	0.1017(16)	0.0051(3)	0.0306(16)	—
,,	0.1547	0.0833(22)	0.0032(3)	0.0274(23)	0.2854(185)

**Table 2.** Lattice data for  $am_\pi$ ,  $am_q$ ,  $aF_\pi$  and  $am_N$ .

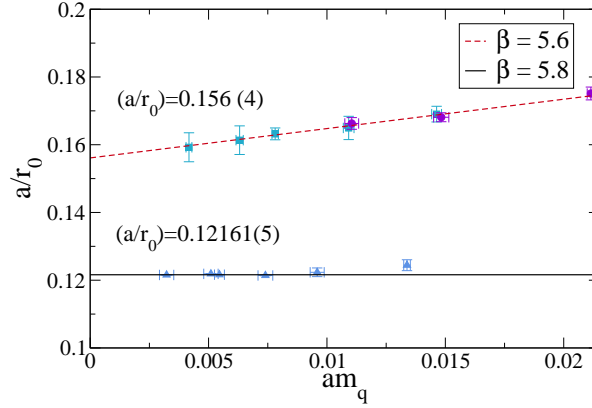


**Figure 5.**  $a/r_0$  versus  $am_q$  at  $\beta = 5.6$  and  $\beta = 5.8$ .

Using the expression for the perturbative lattice Coulomb potential [11, 12]

$$\left[ \frac{1}{R} \right] = \frac{4\pi}{L^3} \sum_{q_i \neq 0} \frac{\cos(aq_i \cdot R)}{4\sin^2(aq_i/2)}, \quad (4.2)$$

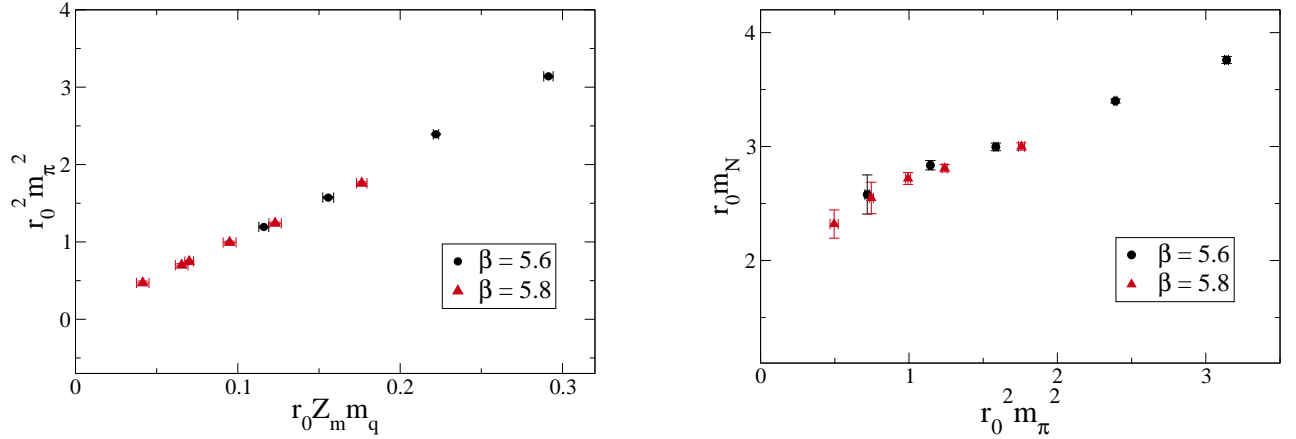


**Figure 6.** Scaling of pion mass squared (left) and nucleon mass (right).

the parametrization of the corrected potential on the lattice reads

$$aV(R) = aV_0 + \tilde{\sigma} R - \frac{\alpha}{R} - \delta_{\text{ROT}} \left( \left[ \frac{1}{R} \right] - \frac{1}{R} \right) \quad (4.3)$$

where  $\delta_{\text{ROT}}$  is the coefficient of the correction term. The measured static potential is fit to the formula in Eq. (4.3) which corrects the lattice data for the lattice artifacts in the Coulomb potential. The first three terms of Eq. (4.3) now gives the continuum potential (i.e., without lattice artifacts). The inverse of the Sommer parameter ( $r_0$ ) in lattice units is calculated using

$$\frac{a}{r_0} = \sqrt{\frac{\tilde{\sigma}}{1.65 - \alpha}}. \quad (4.4)$$

In Fig. 4 we have plotted  $\frac{a}{r_0}$  versus lattice quark mass at  $\beta=5.6$  and 5.8. In the linear fit at  $\beta=5.6$ , we have included  $\kappa=0.15775, 0.158, 0.158125$  in the lattice volume  $24^3 \times 48$  and  $\kappa=0.158, 0.15815, 15825, 0.1583$  in the lattice volume  $32^3 \times 64$ . Similarly at  $\beta=5.8$  the linear fit is done with  $\kappa=0.15445, 0.15455, 0.15462, 0.15466$  and  $0.1547$  in lattice volume  $32^3 \times 64$ . In the chiral limit, the values of  $\frac{a}{r_0}$  obtained are  $0.156(4)$  and  $0.12161(5)$  at  $\beta=5.6$  and 5.8 respectively.

## 5 Cutoff effects

A major source of concern with the use of unimproved Wilson fermions is the potential presence  $\mathcal{O}(a)$  cutoff effects in various observables. In this section we present the cutoff dependence of a variety of observables. In Fig. 6 we have plotted  $(r_0 m_\pi)^2$  (left figure) and  $r_0 m_N$  (right figure) versus  $r_0 Z_m m_q$  and  $(r_0 m_\pi)^2$  respectively using the data at  $\beta=5.6$  and 5.8. Here  $Z_m$  is the quark mass renormalization constant which we have calculated from the  $Z$  factors given in [13]. It is seen that scaling violation are negligible.

In Fig. 7 we have plotted  $r_0 Z_A F_\pi$  versus  $r_0 Z_m m_q$  using the data at  $\beta=5.6$  and 5.8. Data at  $\beta=5.6$ , except at the smallest quark mass, is from lattice volume  $24^3 \times 48$  and the smallest quark

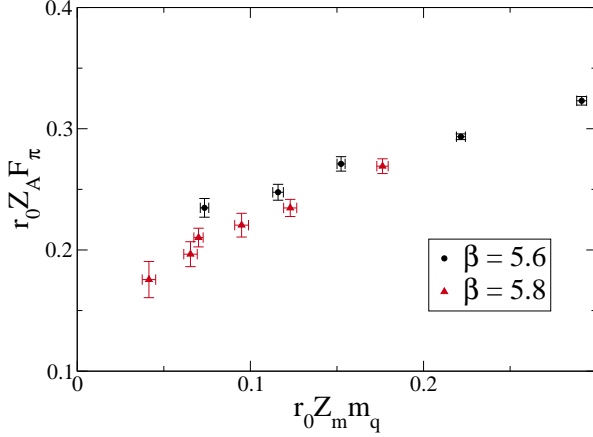


**Figure 7.** Scaling of  $F_\pi$ .

mass data ( $\kappa=0.1583$ ) is from lattice volume  $32^3 \times 64$ . The data at  $\beta=5.8$  is from lattice volume  $32^3 \times 64$ . Note that the physical volume at  $\beta=5.6$  and lattice volume  $24^3 \times 48$  is very close to the physical volume at  $\beta=5.8$  and lattice volume  $32^3 \times 64$ . From the figure it appears that  $F_\pi$  data at  $\beta=5.6$  and  $5.8$  do not exhibit scaling for smaller quark mass region. Since  $F_\pi$  has larger finite volume effect than  $m_\pi$ , the deviation seen at small quark mass region could be partially due to finite volume effects. Note that we have taken the values of non-perturbative renormalization constant  $Z_A$  at  $\beta=5.6$  and  $5.8$  for unimproved Wilson fermions from Ref. [13]. In this reference at  $\beta=5.8$  the lattice volume was  $24^3 \times 48$  and the smallest quark mass probed was greater than 75 MeV. Thus the systematic error in the chiral extrapolation of  $Z_A$  performed in the Ref. [13] at  $\beta=5.8$  may not be properly estimated. Hence the apparent lack of scaling exhibited by  $F_\pi$  may also be partially due to inaccurate determination of  $Z_A$ .

In the scaling region, hadron masses are expected to be independent of the lattice scale and our results demonstrate that they do exhibit very small, if not negligible, cut off dependence in the range of lattice spacings studied.

On the other hand the lattice renormalization constant  $Z_V$  corresponding to the local vector current  $V_\mu^{local}$  which is not conserved for  $a \neq 0$  depends on the lattice spacing and is expected to approach unity as lattice spacing  $a \rightarrow 0$ . In order to verify the expected lattice scale dependence of  $Z_V$  we calculate  $Z_V$  from [14]

$$R_V(t) = \frac{\sum_{k=1}^3 \sum_x \langle \hat{V}_k(x,t) V_k^{local\dagger}(x,t) \rangle}{\sum_{k=1}^3 \sum_x \langle V_k^{local}(x,t) V_k^{local\dagger}(x,t) \rangle} = Z_V + \dots \quad (5.1)$$

with

$$V_\mu^{local}(x) = \bar{q}_i(x) \gamma_\mu q_j(x) \quad (5.2)$$

and (using  $r=1$  throughout in this work)

$$\hat{V}_\mu(x) = \frac{1}{2} [\bar{q}_i(x) (\gamma_\mu - 1) U_\mu(x) q_j(x+\mu) + \bar{q}_i(x+\mu) (\gamma_\mu + 1) U_\mu^\dagger(x) q_j(x)] . \quad (5.3)$$

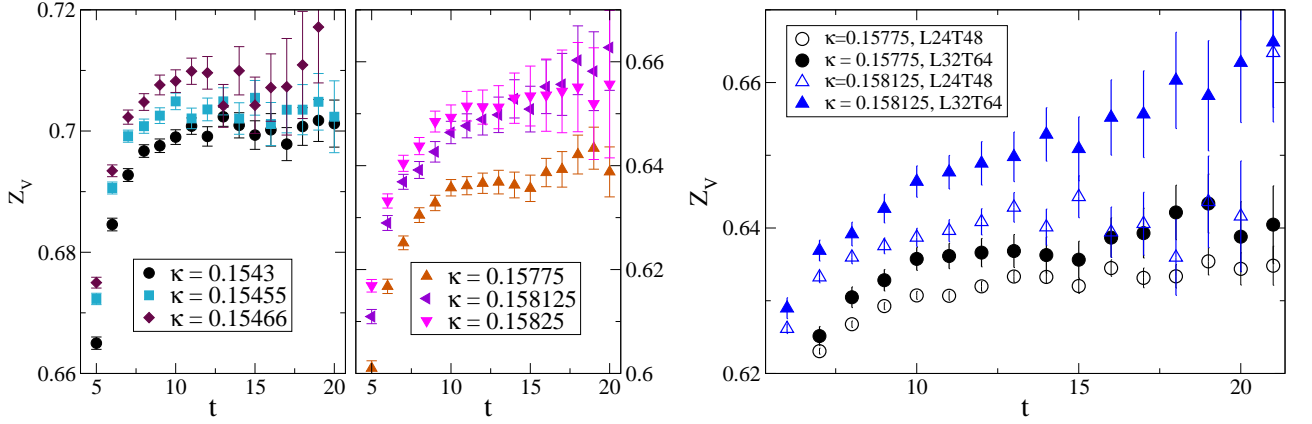


**Figure 8.** Quark mass and scale dependence of  $Z_V$  at L32T64 (left), quark mass and volume dependence of  $Z_V$  at  $\beta = 5.6$  (right).

Our result shown in Fig. 8 (left) exhibits the expected behaviour. On the other hand, finite volume effect on  $Z_V$  is small though not negligible as shown in Fig. 8 (right). As already discussed, in order to examine the cutoff effects in pion decay constant we need accurate determination of  $Z_A$  in the chiral region which is beyond the scope of the present paper.

## 6 Scale determination, chiral behaviour of nucleon mass and extraction of sigma term

To extract the lattice scale, in Fig. 9 we have plotted the ratio  $\frac{m_\pi}{m_N}$  versus  $r_0 m_\pi$ . The data is used to fit the phenomenological formula

$$\frac{m_\pi}{m_N} = a_1 r_0 m_\pi - a_2 (r_0 m_\pi)^3 + a_3 (r_0 m_\pi)^4 \quad (6.1)$$

motivated by baryon chiral perturbation theory. We fit the data at  $\beta=5.8$ , lattice volume  $32^3 \times 64$  and  $\kappa= 0.1543, 0.15445, 0.15455$  and  $0.15462$ . At  $\beta=5.6$ , we use  $\kappa= 0.1575, 0.15775$  in lattice volume  $24^3 \times 48$  and  $\kappa= 0.158, 0.15825, 0.1583$  at lattice volume  $32^3 \times 64$ . Using the physical value of  $\frac{m_\pi}{m_N}$ , we get the intercept of the fitting curve and from the intercept we extract the pion mass in unit of  $r_0$  at the physical point. Now using the value of physical pion mass and the chiral limit of  $\frac{a}{r_0}$ , we have computed lattice spacing  $a$ . The computed values of lattice spacings at  $\beta = 5.6$  and  $5.8$  are  $0.072$  fm and  $0.057$  fm respectively.

We have plotted dimensionfull nucleon mass versus dimensionfull  $m_\pi^2$  in Fig. 10. At  $\beta=5.6$  we have plotted  $\kappa=0.1575, 0.15775$  at lattice volume  $24^3 \times 48$  and  $\kappa= 0.158, 0.15825, 0.1583$  in lattice volume  $32^3 \times 64$ . At  $\beta=5.8$  we have plotted  $\kappa= 0.1543, 0.15445, 0.15455, 0.15462$  and  $0.1547$  in lattice volume  $32^3 \times 64$ . To fit the data we have excluded  $\kappa= 0.1575$  and  $0.1547$  at  $\beta= 5.6$  and  $5.8$  respectively. The data at  $\kappa=0.1575$  is dropped because it is beyond the chiral regime and data at  $\kappa= 0.15475$  has not negligible finite volume effect. We fit the data using baryon chiral perturbation

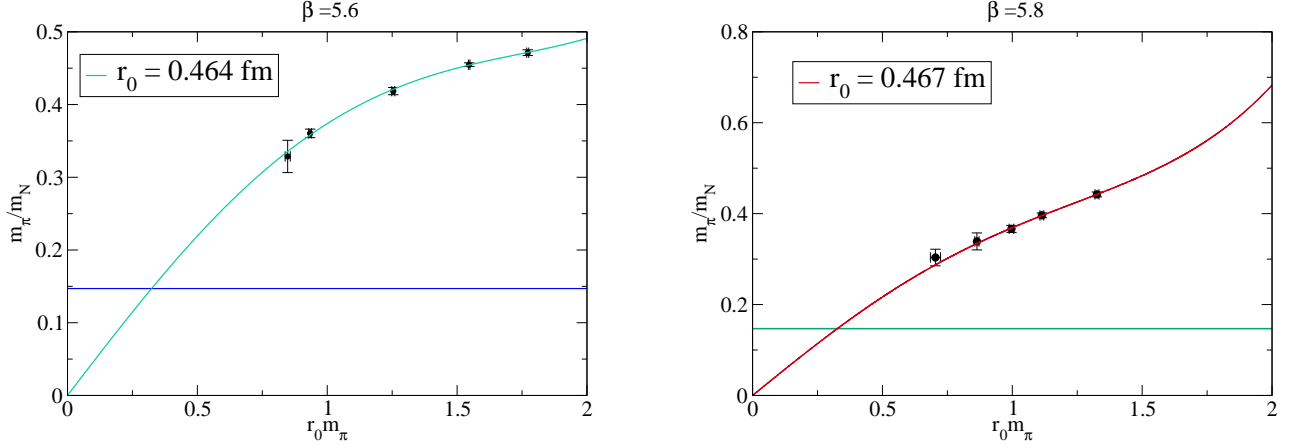


**Figure 9.**  $m_\pi/m_N$  versus  $r_0 m_\pi$  at  $\beta=5.6$  (left) and  $\beta=5.8$  (right)

theory formula to order ( $m_\pi^4$ ) given in Ref. [15]:

$$\begin{aligned}
 M_N = & M_0 - 4c_1 m_\pi^2 - \frac{3g_A^2}{32\pi F_\pi^2} m_\pi^3 + 4e_1^r m_\pi^4 \\
 & + \frac{m_\pi^4}{8\pi^2 F_\pi^2} \left[ \frac{3c_2}{16} - \frac{3g_A^2}{8M_0} + \log \frac{m_\pi}{\lambda} \left( 8c_1 - \frac{3c_2}{4} - 3c_3 - \frac{3g_A^2}{4M_0} \right) \right]. \quad (6.2)
 \end{aligned}$$

For the fit we have treated  $M_0$ ,  $c_1$  and  $e_1^r$  as free parameters and set  $F_\pi = 0.086$  GeV,  $g_A = 1.256$ ,  $c_2 = 3.3$  GeV $^{-1}$ ,  $c_3 = -4.7$  GeV $^{-1}$  and  $\lambda = 1$  GeV. Note that the values of  $c_2$  and  $c_3$  chosen are close to their phenomenological values [15]. The fit along with the error is shown in Fig. 10. The values of the parameters  $M_0$ ,  $c_1$  and  $e_1^r$  we obtain from the fitting are  $M_0 = 0.81(4)$  GeV,  $c_1 = -1.04(5)$  GeV $^{-1}$  and  $e_1^r = 1.2(1)$  GeV $^{-3}$ . Note that the  $c_1$  obtained is close to the phenomenologically determined value [16].

Both from experimental and theoretical point of view, the pion-nucleon  $\sigma$  term is of significant interest. A direct calculation of  $\sigma$  involves the computation of a three point function and is beyond the scope of the present paper. An alternative method of calculation employs Feynman-Hellmann theorem utilizing the dependence of nucleon mass on the quark mass which in turn can be converted into the dependence on pion mass squared. With the parameters used to fit the nucleon data, we calculate the sigma term using the expression [15]

$$\begin{aligned}
 \sigma = & -4c_1 m_\pi^2 - \frac{9g_A^2}{64\pi F_\pi^2} m_\pi^3 + m_\pi^4 \left[ 8e_1^r - \frac{8c_1 l_3^r}{F_\pi^2} + \frac{3c_1}{8\pi^2 F_\pi^2} - \frac{3c_3}{16\pi^2 F_\pi^2} \right. \\
 & \left. - \frac{9g_A^2}{64\pi^2 M_0 F_\pi^2} + \frac{1}{4\pi^2 F_\pi^2} \log \frac{m_\pi}{\lambda} \left( 7c_1 - \frac{3c_2}{4} - 3c_3 - \frac{3g_A^2}{4M_0} \right) \right]. \quad (6.3)
 \end{aligned}$$

where  $l_3^r \equiv -\frac{1}{64\pi^2} \left( \bar{l}_3 + 2 \log \frac{m_\pi^{phys}}{\lambda} \right)$ . In Fig. 11, we plot  $\sigma$  given in Eq. (6.3) together with the error as a function of  $m_\pi^2$  and at physical point  $\sigma = 0.052(4)$  GeV which is compatible with the currently available determinations [15].

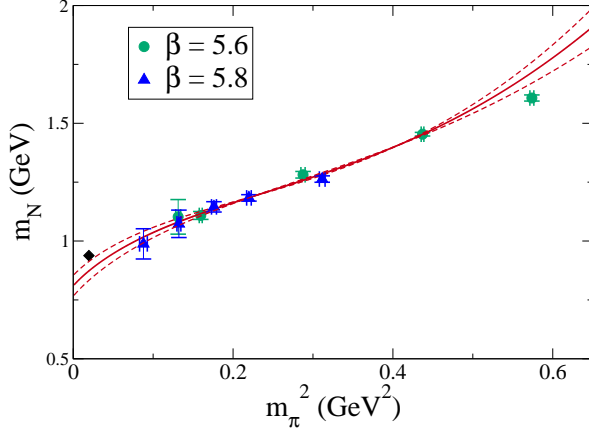


**Figure 10.** Nucleon mass versus  $m_\pi^2$  at  $\beta=5.6$  and  $5.8$ .

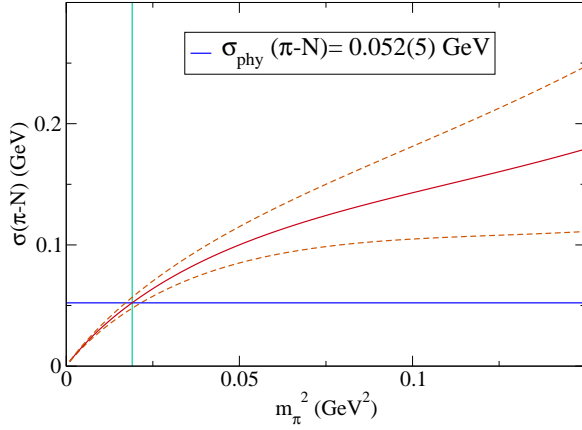


**Figure 11.** Behaviour of the sigma term versus  $m_\pi^2$  at  $\beta=5.6$  and  $5.8$ .

## 7 Chiral extrapolations of pion mass and decay constant and quark condensate

In this section we discuss chiral extrapolation of our data obtained from the pion propagators. In SU(2)  $\chi$ PT at NLO [17], the quark mass ( $r_0 m_q$ ) dependence of  $(r_0 m_\pi)^2$  is given by

$$(r_0 m_\pi)^2 = 2r_0^2 m_q B \left[ 1 - \frac{m_q B}{16\pi^2 F^2} \ln \frac{\Lambda_3^2}{2m_q B} \right] \quad (7.1)$$

where  $F$  is the chiral limit of the pion decay constant and  $B$  and  $\Lambda_3$  are low energy constants. In Fig. 12 we compare our data at  $\beta = 5.6$  and  $5.8$  with a fit to the NLO  $\chi$ PT formula (solid line). For clarity, the LO (dashed line) and the NLO (dot-dashed line) contributions are separately shown. At  $\beta = 5.6$  and lattice volume  $24^3 \times 48$ ,  $\kappa = 0.158$  and  $0.158125$  and at  $\beta = 5.8$  and lattice volume  $32^3 \times 64$ ,  $\kappa = 0.1543$ ,  $0.15445$ ,  $0.15455$ ,  $0.15462$  and  $0.15466$  are used for fitting. The

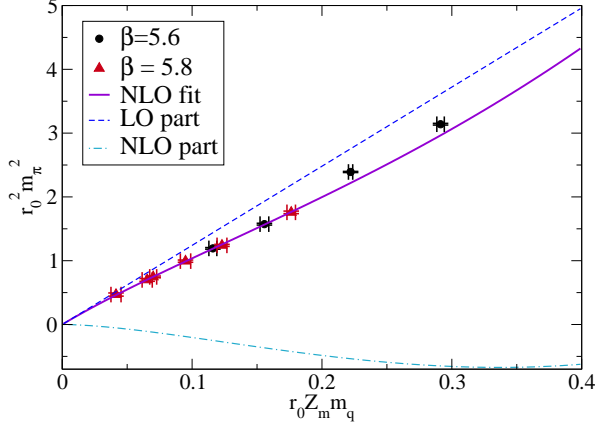


**Figure 12.** NLO chiral perturbation theory fit to  $(r_0 m_\pi)^2$  versus  $r_0 Z_m m_q$ .

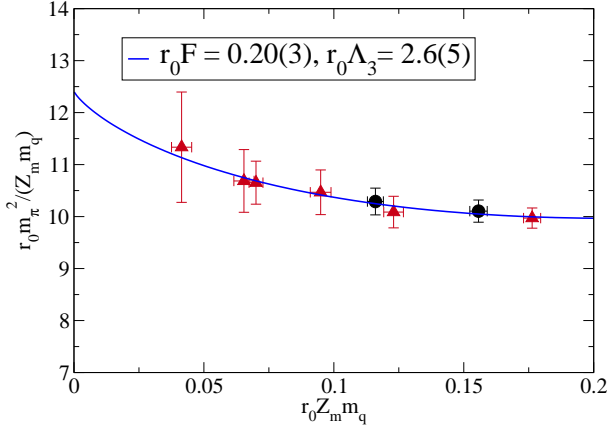


**Figure 13.**  $\frac{r_0 m_\pi^2}{Z_m m_q}$  versus  $r_0 Z_m m_q$  for  $\beta = 5.6$  and  $\beta = 5.8$ .

value of  $F = 86$  MeV is taken as an input. The values of the parameters  $r_0 B$  and  $r_0 \Lambda_3$  obtained from the fit are  $r_0 B = 6.20(13)$  and  $r_0 \Lambda_3 = 2.62(17)$ . Converting these values in physical unit we get  $B = 2651(56)$  MeV and  $\Lambda_3 = 1120(73)$  MeV. Note that the currently available estimates of  $B$  and  $\Lambda_3$  are  $2112 \lesssim B \lesssim 2811$  MeV and  $458 \lesssim \Lambda_3 \lesssim 1020$  MeV [18]. Thus we find that the quark mass dependence of pion mass squared exhibited by our data is in accordance with NLO  $\chi$ PT.

To expose the presence of the chiral logarithm, it is customary to plot

$$\frac{(r_0 m_\pi)^2}{r_0 m_q} = 2r_0 B \left[ 1 - \frac{m_q B}{16\pi^2 F^2} \ln \frac{\Lambda_3^2}{2m_q B} \right] \quad (7.2)$$

We plot  $\frac{(r_0 m_\pi)^2}{r_0 m_q}$  versus  $r_0 Z_m m_q$  in Fig. 13. In the fit, we have used  $r_0 B = 6.2029$  which is obtained from the fit in Fig. 12. The quark masses used in the fit are the same as in Fig. 12.

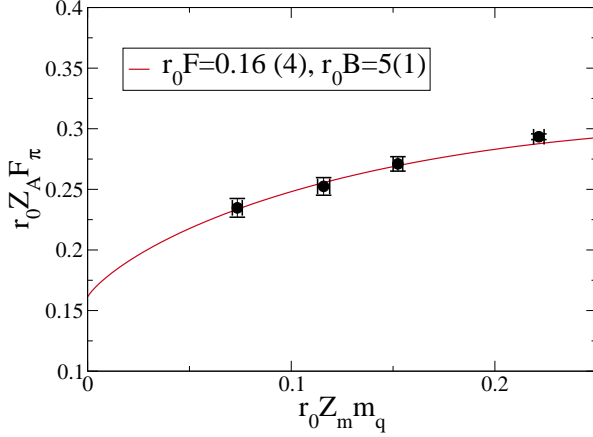


**Figure 14.** Chiral extrapolation of  $r_0 F_\pi$  at  $\beta=5.6$ .

The quark mass dependence of the pion decay constant  $r_0 F_\pi$  in NLO  $\chi$ PT is given by

$$r_0 F_\pi = r_0 F \left[ 1 + \frac{m_q B}{8\pi^2 F^2} \ln \frac{\Lambda_4^2}{2m_q B} \right] \quad (7.3)$$

where  $\Lambda_4$  is another low energy constant. As already mentioned, our renormalized  $F_\pi$  data at  $\beta = 5.8$  has larger uncertainty coming from  $Z_A$  determination and also possible finite volume effects at the smaller quark masses. Therefore we use the data only at  $\beta = 5.6$  for our exploratory chiral extrapolation. In Fig. 14 we compare our data for  $r_0 F_\pi$  versus  $r_0 Z_m m_q$  with NLO  $\chi$ PT at  $\beta=5.6$ . Since  $F_\pi$  has larger finite volume effect compared to  $m_\pi$ , we have used data in lattice volume  $32^3 \times 64$  in this fit. Appropriate to the chiral region, we have used only the lower quark masses ( $\kappa=0.158, 0.15815$  and  $0.1583$ ) for the fit. Since we have fewer points to fit, we have used  $r_0 \Lambda_4 = 3.1134$  ( $\Lambda_4 = 1324$  MeV) (see [18]) as the input to the fit. The upper limits of the values obtained for  $F$  and  $B$  (see Fig. 14) are close to the currently accepted values [18]. Note however that there is some uncertainty arising from the value of  $Z_A$ . Thus in the case of  $F_\pi$  it is safe to say that our data is not incompatible with NLO  $\chi$ PT prediction. However simulations at smaller quark masses with less systematic errors due to finite volume and  $Z_A$  determination is needed to reach a definite conclusion.

Next we consider the extraction of chiral condensate from our data. In continuum limit, the effect of Wilson term on chiral condensate does not vanish because Wilson term is a dimension five operator. In other words, it renormalizes the chiral condensate additively, in addition to multiplicatively. Thus in the case of Wilson fermions, a direct measurement of the quark condensate on the lattice and then taking the chiral continuum limit will not give the desired condensate. The well-known alternate procedure to calculate the chiral condensate on the lattice with Wilson fermions is utilizing chiral Ward-Takahashi identities [19, 20]

$$\langle \bar{\psi} \psi \rangle \delta^{ab} = 2 m_q \int d^4 x \langle P^a(x) P^b(0) \rangle \Rightarrow \langle \bar{\psi} \psi \rangle = 2 m_q \frac{C_{PP}}{m_\pi} = C_{AP} \quad (7.4)$$

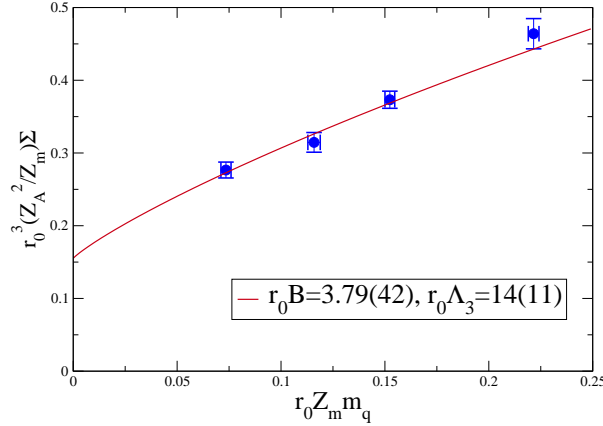


**Figure 15.** Renormalized quark condensate versus renormalized PCAC quark mass at  $\beta = 5.6$  in unit of  $r_0$ .

using Eq. (2.10). In Fig. 15 we plot the chiral behaviour of the quark condensate ( $\Sigma$ ) together with an NLO fit at  $\beta=5.6$  and lattice volume  $32^3 \times 64$ . According to NLO  $\chi$ PT

$$\Sigma = F^2 B \left[ 1 - \frac{3Bm_q}{16\pi^2 F^2} \ln\left(\frac{2Bm_q}{\Lambda_3^2}\right) \right] \quad (7.5)$$

The quark masses used are as in Fig. 14. In this fit we have used the chiral limit of  $r_0 F = 0.20$  (corresponds to  $F = 86$  MeV) as input. The value of chiral condensate obtained from the fit is  $\Sigma^{1/3} = 228(8)$  MeV. Note that since the values of  $F_\pi$  have entered the determinations of condensates all the caveats that we have mentioned in the context of chiral extrapolation of  $F_\pi$  apply in this case also.

## 8 Summary

We have calculated pion mass, pion decay constant, PCAC quark mass and nucleon mass in two flavour lattice QCD with unimproved Wilson fermion and gauge actions. Simulations are performed using DD-HMC algorithm at two lattice spacings and two volumes for several values of the quark mass. The cutoff effects in pion mass and nucleon mass for the explored region of parameter space are found to be negligible. The chiral behaviours of pion mass, pion decay constant and quark condensate are found to be qualitatively consistent with NLO chiral perturbation theory.

### Acknowledgements

Numerical calculations are carried out on Cray XD1 and Cray XT5 systems supported by the 10th - 12th Five Year Plan Projects of the Theory Division, SINP under the DAE, Govt. of India. We thank Richard Chang for the prompt maintenance of the systems and the help in data management. This work was in part based on the public lattice gauge theory codes of the MILC collaboration [21] and Martin Lüscher [3].

## References

- [1] K. G. Wilson, Phys. Rev. **D10**, 2445-2459 (1974); K. G. Wilson, “Quarks and Strings on a Lattice”, in *New Phenomena in Subnuclear Physics*, Proceedings of the International School of Subnuclear Physics, Erice, 1975, edited by A. Zichichi (Plenum, New York, 1977).
- [2] L. Del Debbio, L. Giusti, M. Luscher, R. Petronzio and N. Tantalo, JHEP **0602**, 011 (2006).
- [3] M. Lüscher, Comput. Phys. Commun. **156**, 209-220 (2004). [hep-lat/0310048]; M. Lüscher, Comput. Phys. Commun. **165**, 199-220 (2005). [hep-lat/0409106].  
<http://luscher.web.cern.ch/luscher/DD-HMC/index.html>
- [4] A. K. De, A. Harindranath and S. Mondal, Phys. Lett. B **682**, 150 (2009) [arXiv:0910.5611 [hep-lat]].
- [5] A. K. De, A. Harindranath and S. Mondal, JHEP **1107**, 117 (2011) [arXiv:1105.0762 [hep-lat]].
- [6] A. Chowdhury, A. K. De, S. De Sarkar, A. Harindranath, S. Mondal, A. Sarkar and J. Maiti, Phys. Lett. B **707**, 228 (2012) [arXiv:1110.6013 [hep-lat]].
- [7] A. Chowdhury, A. K. De, S. De Sarkar, A. Harindranath, S. Mondal, A. Sarkar and J. Maiti, PoS LATTICE **2011**, 099 (2011) [arXiv:1111.1812 [hep-lat]].
- [8] A. Chowdhury, A. K. De, A. Harindranath, J. Maiti and S. Mondal, JHEP **1211**, 029 (2012) [arXiv:1208.4235 [hep-lat]].
- [9] A. Chowdhury, A. K. De, S. De Sarkar, A. Harindranath, J. Maiti, S. Mondal and A. Sarkar, arXiv:1209.3915 [hep-lat].
- [10] A. Hasenfratz, F. Knechtli, Phys. Rev. **D64**, 034504 (2001). [hep-lat/0103029].
- [11] C. B. Lang and C. Rebbi, Phys. Lett. B **115**, 137 (1982).
- [12] C. Michael, Phys. Lett. B **283**, 103 (1992) [arXiv:hep-lat/9205010].
- [13] D. Becirevic, B. Blossier, P. Boucaud, V. Gimenez, V. Lubicz, F. Mescia, S. Simula and C. Tarantino, Nucl. Phys. B **734**, 138 (2006) [hep-lat/0510014].
- [14] L. Maiani and G. Martinelli, Phys. Lett. B **178**, 265 (1986).
- [15] G. S. Bali, P. C. Bruns, S. Collins, M. Deka, B. Glasle, M. Gockeler, L. Greil and T. R. Hemmert *et al.*, Nucl. Phys. B **866**, 1 (2013) [arXiv:1206.7034 [hep-lat]].
- [16] V. Bernard, N. Kaiser and U. -G. Meissner, Nucl. Phys. A **615**, 483 (1997) [hep-ph/9611253].
- [17] J. Gasser and H. Leutwyler, Annals Phys. **158**, 142 (1984).
- [18] G. Colangelo, S. Durr, A. Juttner, L. Lellouch, H. Leutwyler, V. Lubicz, S. Necco and C. T. Sachrajda *et al.*, Eur. Phys. J. C **71**, 1695 (2011) [arXiv:1011.4408 [hep-lat]].
- [19] M. Bochicchio, L. Maiani, G. Martinelli, G. C. Rossi and M. Testa, Nucl. Phys. B **262**, 331 (1985).
- [20] L. Giusti, F. Rapuano, M. Talevi and A. Vladikas, Nucl. Phys. B **538**, 249 (1999) [hep-lat/9807014].
- [21] <http://physics.indiana.edu/~sg/milc.html>